Cell Reports
Physical Science

Article

Encapsulation of hydrophobic pollutants within a large water-soluble $[Fe_4L_6]^{4-}$ cage

Graphical abstract

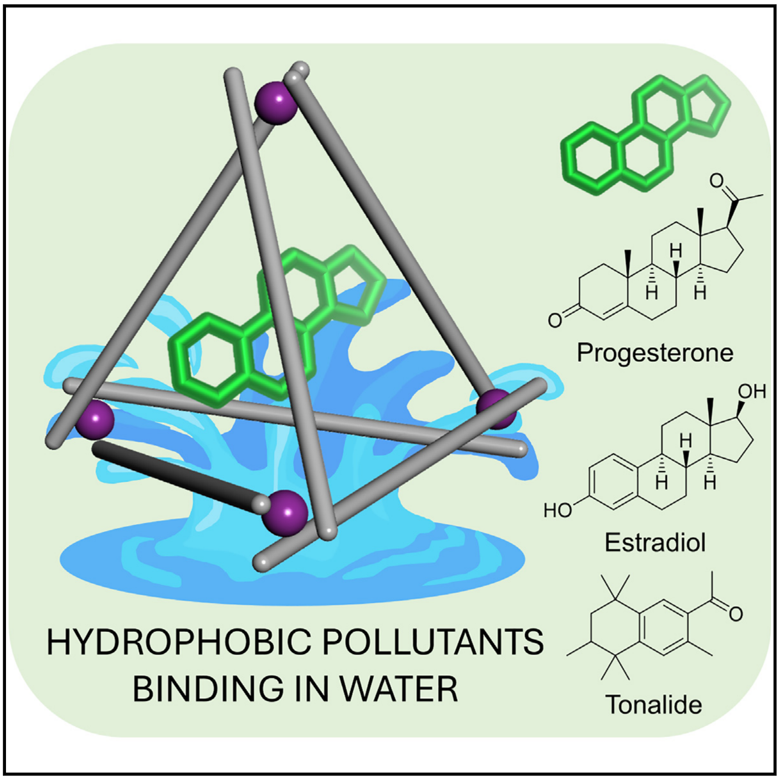

Authors

Jack D. Wright, George F.S. Whitehead, Edward O. Pyzer-Knapp, Imogen A. Riddell

Correspondence

imogen.riddell@manchester.ac.uk

In brief

Metal-organic cages remain underexplored for host-guest binding in aqueous media due to challenges associated with synthesizing water-stable cages. Here, Wright et al. report the synthesis of a large (657 Å^3) water-soluble Fe_4L_6 tetrahedron via the introduction of solvating sulfonate moieties. The tetrahedron can bind polycyclic hormones and other wastewater pollutants.

Highlights

- An adaptable synthesis for production of water-soluble metal-organic cages
- Binding of wastewater pollutants, including medicinal and healthcare products
- Isothermal titration calorimetry (ITC)-derived host-guest binding constants
- Data-driven identification of key physical properties dictating host-guest binding

Wright et al., 2025, Cell Reports Physical Science 6, 102404
February 19, 2025
https://doi.org/10.1016/j.xcrp.2025.102404

Cell Reports
Physical Science

CellPress
OPEN ACCESS

Article

Encapsulation of hydrophobic pollutants within a large water-soluble $[Fe_4L_6]^{4-}$ cage

Jack D. Wright,[1] George F.S. Whitehead,[1] Edward O. Pyzer-Knapp,[2,3] and Imogen A. Riddell[1,4,*]
[1]Department of Chemistry, The University of Manchester, Oxford Road, Manchester M13 9PL, UK
[2]IBM Research Europe, Daresbury, UK
[3]Present address: Xyme, 22 St John's Street, Manchester M3 4EB, UK
[4]Lead contact
*Correspondence: imogen.riddell@manchester.ac.uk
https://doi.org/10.1016/j.xcrp.2025.102404

SUMMARY

Hydrophobic molecules lost in water systems can have significant impacts on local ecology. Notably, the discharge of unmetabolized medications, specifically hormones, and hygiene products into effluent wastewater is a pressing environmental challenge. While selective capture of these molecules has been demonstrated by metal-organic cages (MOCs), these studies typically employ an organic solvent system that does not reflect aqueous environmental conditions. In this study, we report a rare, water-soluble, tetrahedral MOC bearing hydrosolvating sulfonate moieties alongside an aromatic naphthyl spacer. The MOC encloses a large (657 $Å^3$) cavity that can bind a range of polycyclic structures in aqueous media. Isothermal titration calorimetry measurements support guest binding being an enthalpically driven hydrophobic binding process. The synthetic strategy employed to prepare the MOC is extensible and thus serves as a promising route to a range of large, water-soluble MOCs containing hydrophobic binding cavities with exciting prospects.

INTRODUCTION

Contamination of natural waterways by exogenous, hydrophobic pollutants is known to have an adverse effect on the local ecology.[1] In particular, there has been growing concern over residual hormone levels rising due to unmetabolized medications entering wastewater streams and causing unintended biological consequences to both humans and animals.[2] Similarly, chemicals such as tonalide, a base scent in perfumes, are increasingly entering waste streams and are now widely recognized to harm the surroundings.[3–5] Selective binding[6,7] and subsequent removal of these marginally water-soluble molecules provides an attractive route to ameliorate the environmental impact of these compounds.[8]

Water-soluble coordination cages are a promising approach for selective binding,[9,10] having previously demonstrated the capture and storage of the greenhouse gas SF_6 and chemical warfare agents.[11–13] Significantly fewer examples of water-soluble metal-organic cages (MOCs) have, however, been reported to date compared with their organo-soluble counterparts.[14] This reflects challenges with the aqueous solubility of the aromatic paneled ligands, which are typically employed to span the metal vertices in these complexes.[15–18] Through prescient ligand design, the structure of MOCs and their associated void spaces has been tuned, leading to the development of a wide range of applications, including catalysis,[19] molecular recognition,[20] and labeling.[21] There are, however, clear additive benefits to the synthesis of water-soluble cages, namely the ability to utilize the hydrophobic effect for the binding of a broad range of molecules with high affinity,[22] as well as the potential application of water-soluble cages in bioimaging and drug delivery.[23–25]

Current strategies for the development of aqueous cages rely heavily on the use of kinetically inert metal ions[26,27] or the retroactive induction of water solubility to convert organic soluble complexes, through anion exchange, into water-soluble cages, which have limited stability over longer timescales.[28] There are few consistent methods of invoking aqueous solubility as a part of MOC design.[29] In this study, we report the synthesis of a water-soluble MOC designed with solvating groups and employing a synthetic approach that may be transferred to other established ligand systems. We show that the $[Fe_4L_6]^{4-}$ tetrahedron (**C1**) formed can bind a range of hydrophobic guests, including manmade pollutants recognized to have significant detrimental effects upon introduction into wastewater streams (Figure 1).

RESULTS AND DISCUSSION

To ensure the formation of a water-soluble MOC, the solubility of the precursor ligand was actively considered from the outset. We also estimated that an M_4L_6 cage with a void cavity of approximately 527 $Å^3$, corresponding to an M–M distance of 16.5 Å, was required based on a 55% fill volume[30] when targeting the binding of progesterone, ethinylestradiol, and tonalide in water (Note S4.1.2). Evaluation of the literature,[31] alongside the availability of **1a** as a commercial precursor, identified **L1** as a potential subcomponent synthetically accessible via a sultone ring-opening reaction. Sulfonate-based ligands have previously

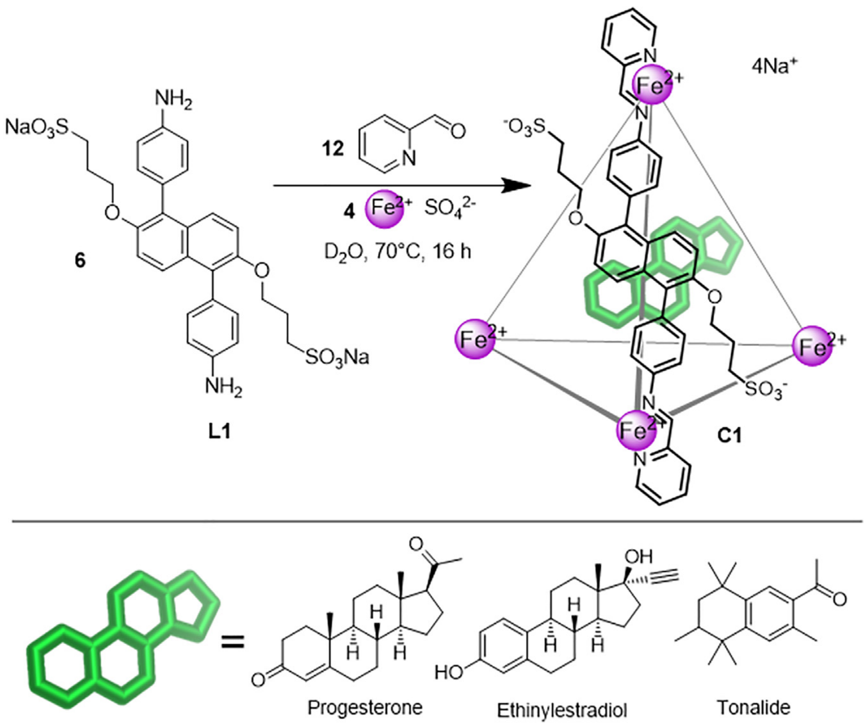

Figure 1. Subcomponent self-assembly of C1

Synthesis occurs from **L1** (6 equiv), 2-formylpyridine (12 equiv), and iron(II) sulfate (4 equiv) in water. The initial guests targeted for encapsulation (progesterone, ethinylestradiol, and tonalide) are represented by the green general polycyclic structure.

been shown to have good aqueous solubility and be compatible with iron(II)-based self-assembly strategies.[32] Moreover, once formed, the iron(II) structure displays versatile applications due to the well-defined hydrophobic binding pocket. The impact of this approach has, however, been limited by the commercial availability of ligands, which has restricted its generalization. Here, we overcome this limitation, demonstrating the facile installation of sulfonate moieties on hydroxyl-functionalized ligand precursors.

Sulfonate ligand synthesis

Synthesis of the diamino ligand (**L1**) was achieved following a two-step procedure (Scheme 1) comprising a ring-opening addition of 1,3-propanesultone[33] with 1,5-dibromonaphthalene-2,6-diol (**1a**). The subsequent dibrominated spacer (**1b**) underwent a Pd-catalyzed Suzuki-Miyaura cross-coupling with commercially available 4-aminophenylboronic acid pinacol ester under standard conditions[34] to produce the diamino ligand (**L1**). The disodium sulfonate salt (**L1**) was water soluble and easily purified by recrystallization, facilitating larger gram-scale synthesis without the need for scale- and time-limited purification techniques such as high-performance liquid chromatography (HPLC).[35] Following recrystallization, the formation of **L1** was confirmed by conventional nuclear magnetic resonance (NMR) and mass spectrometry (MS) analyses, and the purity was confirmed by elemental analysis (Figures S5–S9).

Assembly and characterization of MOC C1

We next explored the self-assembly of the C_2-symmetric ligand, **L1**, with iron(II) sulfate. Given its structural similarity to the reported ligands, we predicted that an Fe_4L_6 tetrahedron would form, noting that the horizontal orientation of the naphthyl spacer reduces the likelihood of M_2L_3 helicates being formed as a side product.[36] Immediately upon mixing 4 equiv of iron(II) sulfate heptahydrate, 12 equiv of 2-formylpyridine, and 6 equiv of **L1** in D_2O, a turbid purple solution was generated. After heating at 70°C for 12 h, a clear purple solution was obtained, indicative of low-spin iron(II) pyridylimine bond formation. The ^{1}H-NMR spectrum (Figure S11) also supported the formation of a diamagnetic complex with multiple environments observed per ligand resonance. Closer inspection of the ^{1}H-NMR spectrum and deconvolution of the proton resonances in the 9–9.5 ppm region supported the formation of a mixture of Fe_4L_6 tetrahedra in T (20%), C_3 (35%), and S_4 (45%) configurations (Figure S11). The formation of diastereoisomeric mixtures of tetrahedra is frequently observed when an extended organic linker, which has more degrees of freedom, is employed.[34,37] More flexible ligands facilitate the incorporation of a mixture of Λ- and Δ-isomers around the octahedral metal centers, and in solution, an equilibrium of achiral S_4 (ΛΛΔΔ), heterochiral C_3 (ΛΔΔΔ/ΔΛΛΛ), and homochiral T (ΛΛΛΛ/ΔΔΔΔ) symmetric cages can be observed.[38] Further support for the formation of a diastereoisomeric mixture of Fe_4L_6 tetrahedra (**C1**) was obtained by MS and diffusion-ordered spectroscopy (DOSY), neither of which provided any indication for the formation of an M_2L_3 helicate (Figures S13 and S17). A single diffusion coefficient (D) corresponding to all the proton resonances was found for **C1**; at 1.62×10^{-10} cm^2s^{-1}, this corresponds to a hydrodynamic radius of 15.1 Å and is comparable with analogous, organic-soluble systems reported in the literature.[34] **C1** could be isolated in high yields as a purple powder, which can be readily redissolved in water. A comparison between ^{1}H-NMR spectra of **C1** made *in situ* and **C1** redissolved following isolation indicates no significant changes between the structures of **C1** (Figure S11).

Following the slow diffusion of dioxane into an aqueous solution of **C1**, suitable single crystals for X-ray diffraction were obtained (Figure 2). Refinement of the diffraction data revealed that the predicted Fe_4L_6 tetrahedron had formed, with the achiral S_4 symmetric structure incorporating two Λ and two Δ coordinated metal centers, exclusively observed in the crystal structure. The alkyl sulfonates are orientated away from the central cavity, which is a hydrophobic binding pocket bounded by the aromatic naphthyl units. As the sulfonates orientate to maximize

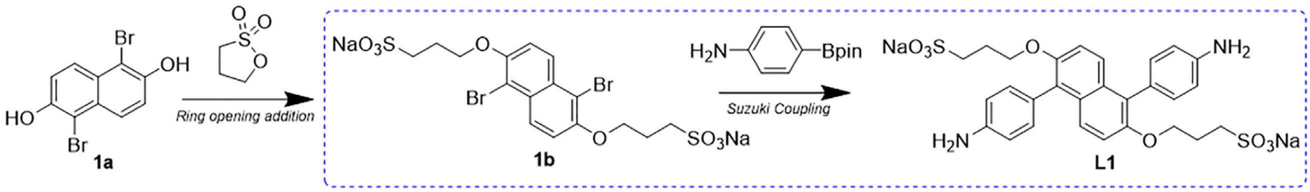

Scheme 1. Stepwise synthesis of water-soluble ligand L1 from a dibromonaphthalene derivative, 1a, via dibromo spacer compound, 1b
Compounds within the blue dashed box all show sulfonate-aided solubility in water.

hydrogen-bonding interactions with the solvent water of crystallization, the alkyl chains narrow the cage pore (Figure S56), increasing the degree of enclosure of **C1**.[34] Void space calculations on **C1** using VOIDOO[39] revealed a cavity volume of 657 Å^3, which, like the average M–M bond length (17.2 Å), is slightly larger than our initial target (Figure 2B). While many tetrahedra with similarly sized internal cavities have been reported,[34] exceptionally few are water soluble and incorporate dynamic metal bonds.[29] Cage **C1** is thus an exciting water-soluble host molecule with the capacity to bind polycyclic guests through π–π stacking and hydrophobic interactions. The single-crystal structure gives insight into the internal and interfacial environments of **C1** and how it may interact with guests and bulk media.

Host-guest binding studies

Having confirmed the structure of **C1**, we next tested its potential for guest binding against our target molecules—progesterone, ethinylestradiol (the estradiol derivative employed in contraceptives[41]), and tonalide. Based on previous data analysis of a smaller water-soluble iron(II) pyridyl imine cage that identified logP as the primary factor for guest binding and volume as a secondary parameter, we predicted that **C1** would act as a suitable host for each of the hydrophobic molecules targeted (Note S4). The initial ^{1}H-NMR spectra, where progesterone, ethinylestradiol, or tonalide had been added to separate solutions of **C1**, supported each of the guests' binding (Note S5). Each of these potential guests is insoluble in pure D_2O (Figure S20) but could clearly be observed through a new set of peaks in the −2 to 1.5 ppm region when in solution with **C1**. The upfield shift of the alkyl proton signals, relative to each of the guests in acetonitrile-d_3 (Figure S20), is indicative of binding inferred to be stabilized between the encapsulated guests and the naphthyl paneling of the cavity within **C1**. Moreover, examination of the specific resonances for each host-guest complex suggests changes in the diastereomeric mixture of the cages upon binding. For progesterone$\subset$**C1**, the imine region appears to simplify, while for tonalide$\subset$**C1**, close examination of the tonalide resonances reveals more ^{1}H-NMR peaks than expected for the guest, which is indicative of tonalide binding within a lower symmetry cage. Host-guest binding was also supported by the consistent diffusion coefficients seen between the host and guest

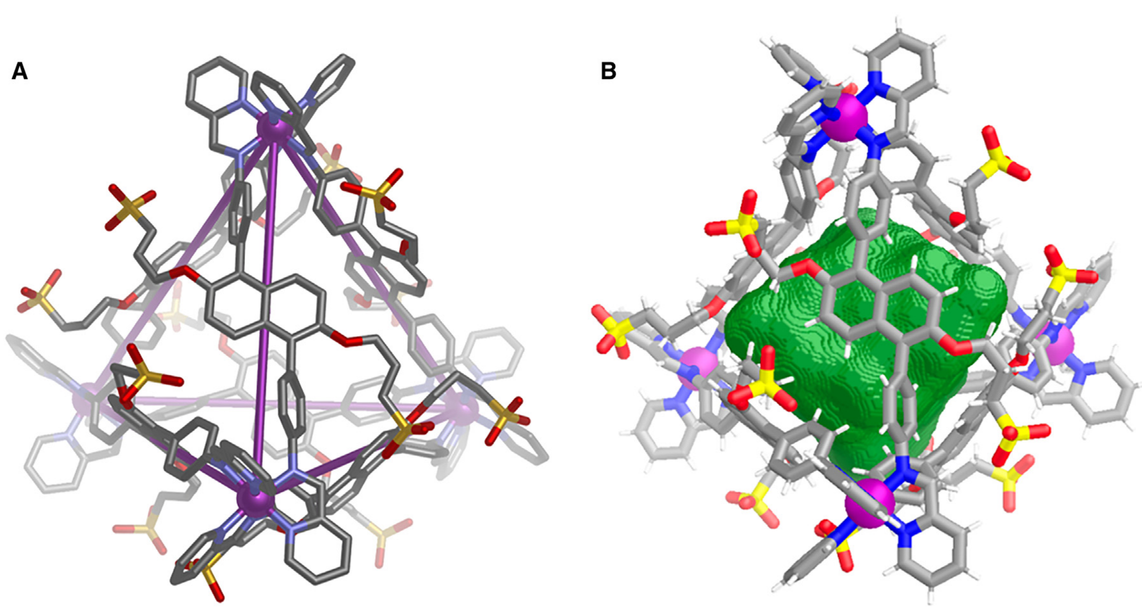

Figure 2. Single-crystal X-ray structure of C1
(A) Hydrogen atoms, solvent, and disorder have been omitted for clarity. Fe(II) ions (purple), O atoms (red), S atoms (yellow), N atoms (blue), and C atoms (gray). No evidence of sodium counter cations was observed in the crystal structure, leading us to postulate that four of the twelve sulfonate moieties were protonated during crystallization.
(B) VOIDOO[40]-calculated void space (shown using green mesh) within the structure of **C1**.

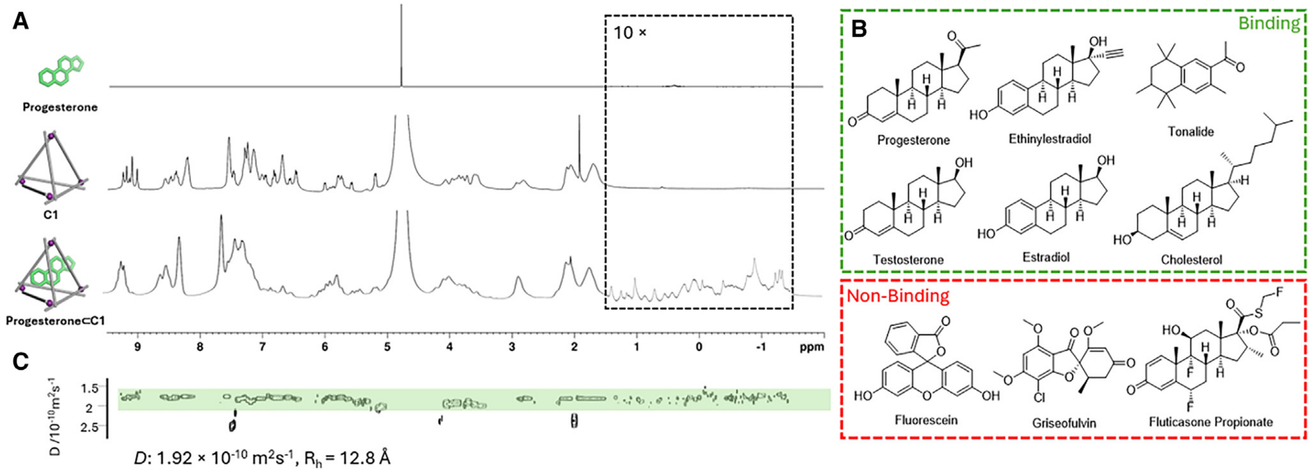

Figure 3. Characterization of host-guest complex between C1 and progesterone

(A) ^{1}H-NMR (500 MHz, D_2O, 298 K) of **C1** and progesterone ⊂ **C1**; peaks in the dashed box have been scaled 10-fold for clarity and correspond to the proton environments of encapsulated progesterone. In the absence of **C1**, no progesterone could be detected by ^{1}H-NMR under any conditions.

(B) Hydrophobic guests tested for binding within **C1**: guests in the green box were shown to bind, while those in the red box did not show evidence of binding.

(C) ^{1}H DOSY analysis of progesterone ⊂ **C1** (400 MHz, D_2O, 298 K). A diffusion coefficient of 1.92×10^{-10} m^2s^{-1} was recorded across host and guest resonances, giving a hydrodynamic radius of 12.8 Å.

resonances in DOSY NMR (Figure 3). Additionally, changes were observed in the ^{1}H-NMR spectra in the imine region (9.5–8.9 ppm) consistent with host-guest formation, and nuclear Overhauser effect (NOE) peaks between the ^{1}H resonances of each of the guests and protons on the naphthyl ring of **C1** (Note S5) were observed. Finally, evidence for host-guest formation was also obtained by MS, where *m/z* peaks correlating with [guest ⊂ **C1**]$^{4-}$ were observed. Property analysis of progesterone, ethinylestradiol, and tonalide revealed predicted logP values spanning 3.61–4.72 and volumes of between 259 and 320 Å^3, reflecting percentage fill volumes of 39%–49%. Based on these values, we expanded our potential range of guests further to include testosterone (predicted logP = 3.87; vol = 292 Å^3), estradiol (predicted logP 3.61; vol = 269 Å^3), cholesterol (predicted logP = 7.39; vol = 423 Å^3), fluorescein (predicted logP = 3.66; vol = 276 Å^3), griseofulvin (predicted logP = 2.81; vol = 297 Å^3), and fluticasone propionate (predicted logP = 4.43, vol = 435 Å^3) (Table S1). Potential guests were chosen based on similarities in their structures and properties to progesterone, as well as their recognized status as pollutants. Analysis of reaction mixtures of each of these potential guests with **C1** revealed that estradiol, testosterone, and cholesterol also bound, being both hydrophobic and of an appropriate size. Interestingly, progesterone has previously been reported to bind within a MOC in acetonitrile; however, that system did not bind cholesterol.[42]

In contrast, griseofulvin, an antifungal medicine with a low logP value, was not observed to bind, nor were fluorescein (pH 7.45) or fluticasone propionate, a common antiinflammatory drug.[43,44] While the lack of binding of fluticasone propionate, which has a similar polycyclic ring system to progesterone and an appropriate logP value, can be attributed to the increased volume of the guest, the observation that fluorescein does not bind is not predicted based on logP and volume calculations. The lack of fluorescein binding within **C1** most likely reflects that progesterone has a planar ring system, while fluorescein does not, and thus volume is too trivial a descriptor when polycycles are included as guest molecules. The initial model was based on a smaller cage, which did not accommodate polycyclic guests.

Next, we set out to determine the binding constants for progesterone, ethinylestradiol, tonalide, testosterone, and estradiol within **C1**. Due to the complexity of the ^{1}H-NMR spectra, which were not simplified by heating or inclusion of the guest, we explored the use of isothermal titration calorimetry (ITC; Figure 4; Note S6) to extract binding constants. Due to the hydrophobic nature of the guests, binding could not be assessed in a pure aqueous solution and titrations had to be completed in a 1:1 water:methanol solution to ensure full solvation of the guest molecules throughout the titration. Cholesterol displayed limited solubility even when in a mixed 1:1 water:methanol solution in the absence of **C1**, and so no binding constant was obtained. Analysis of the ITC data for each of the host-guest systems revealed binding constants ranging from 1.4 to 28 × 10^4 M^{-1}. For each of the titrations, binding was also found to be enthalpically driven (supplemental notes; Table S2), consistent with behavior observed for other water-soluble supramolecular hosts employing hydrophobic binding.[45,46] Thus, while practically, the use of a 1:1 water:methanol solution was required for ITC measurements, higher binding constants are predicted in pure water.

In conclusion, we have successfully synthesized a water-soluble MOC using a simple, high-yielding ring-opening addition to introduce water-soluble sulfonate moieties into the ligands prior to complexation. The water-soluble MOC (**C1**) incorporates a large cavity that is able to bind a range of polycyclic molecules in water with high affinity. Among the guests investigated, ethinylestradiol and tonalide are particularly noteworthy due to their recognized status as environmental pollutants. Our results thus highlight how a solubility-first approach to ligand design can allow access to water-soluble cages with large cavities and

A

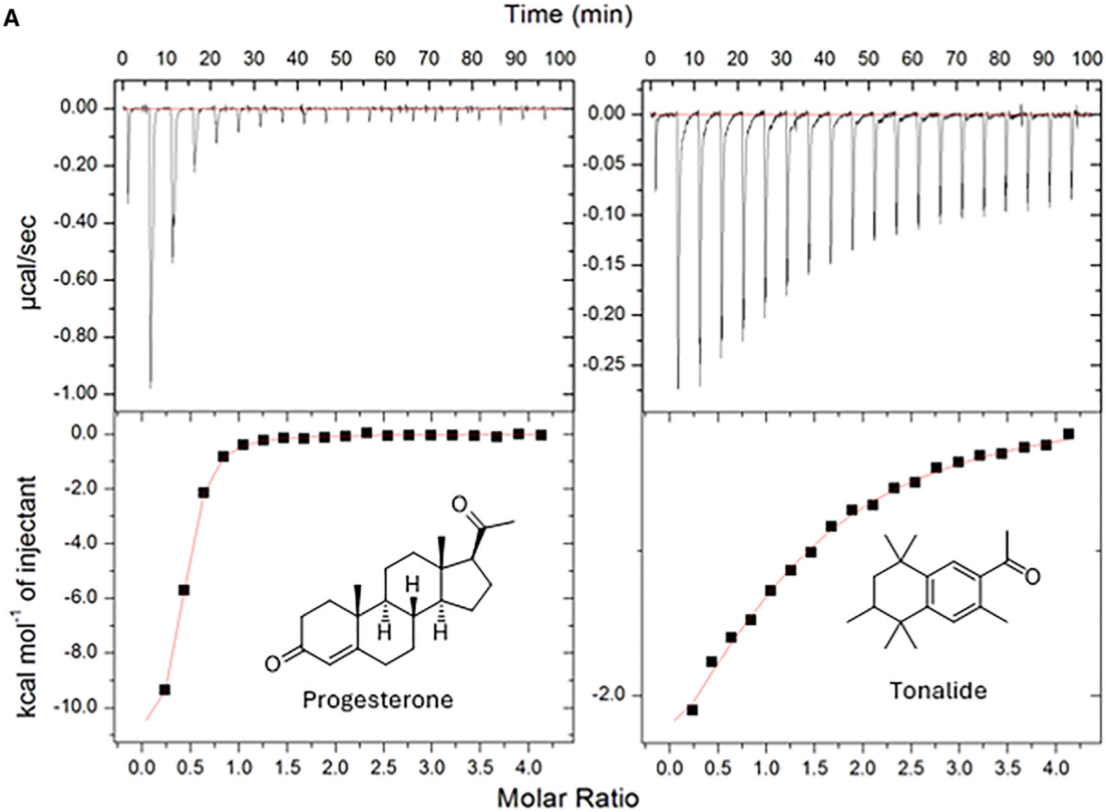

B

Guest	K_a (M^{-1})	LogP	Volume (Å³)	C1 % Fill Volume
Ethinylestradiol	28×10^4 ($\pm 5.9 \times 10^4$)	3.61	291.1	44%
Progesterone	24×10^4 ($\pm 0.9 \times 10^4$)	4.72	319.6	49 %
Testosterone	21×10^4 ($\pm 1.7 \times 10^4$)	3.88	292.1	44 %
Tonalide	1.4×10^4 ($\pm 0.2 \times 10^4$)	4.48	259.1	39 %
Estradiol	1.0×10^4 ($\pm 0.1 \times 10^4$)	3.61	268.7	41%

Figure 4. ITC data for host-guest binding of C1

(A) Isothermal titration calorimetry (ITC) spectra recording the host-guest binding of progesterone (top left) and ethinylestradiol (top right) with **C1** in water: methanol (1:1 v/v). The integrated heat of encapsulation plotted against the H:G molar ratio enabled the extraction of the binding constant, K_a (bottom).

(B) Guests and their respective binding constants, logP values, volumes, and percentage fill of **C1**. All binding constants were measured in triplicate. Data are represented as mean ± standard error.

strong hydrophobic driving forces and supports ongoing efforts to develop clean supramolecular catalysts as well as biological applications for MOCs.

METHODS

All synthesis and characterization can be found in the supplemental notes. For complete synthetic and experimental procedures, alongside further details regarding the methods, refer to the supplemental notes.

RESOURCE AVAILABILITY

Lead contact

Further information and requests for resources should be directed to and will be fulfilled by the lead contact, Imogen A. Riddell (imogen.riddell@manchester.ac.uk).

Materials availability

Request for materials generated in this study should be sent to the lead contact, Imogen A. Riddell.

Data and code availability

- Single crystallographic data have been deposited at the Cambridge Crystallographic Data Center as deposition number CCDC: 2373788 and are publicly available as of the date of publication. This deposition number contains the supplementary crystallographic data for this paper. These data are provided free of charge by the joint Cambridge Crystallographic Data Centre and Fachinformationszentrum Karlsruhe Access Structures service.
- All original code has been deposited at Zenodo at https://doi.org/10.5281/zenodo.14599103 and is publicly available as of the date of publication.
- Any additional information required to reanalyze the data reported in this paper is available from the lead contact upon request.

ACKNOWLEDGMENTS

This work was supported by a The Royal Society (UK) University Research Fellowship (IAR; URF\R1\180414), including a contribution to a PhD studentship (J.D.W.). We also thank the EPSRC and NMR infrastructure (EP/K039547/1 and EP/R00482X/1) and the Diamond Light Source for access to synchrotron X-ray facilities at Beamline I-19 (cy31541). I.A.R. and J.D.W. also thank Prof. Simon Webb for helpful discussions and gift of ethinylestradiol.

AUTHOR CONTRIBUTIONS

Conceptualization, J.D.W., E.O.P.-K., and I.A.R.; methodology, J.D.W. and E.O.P.-K.; software, E.O.P.-K.; formal analysis, J.D.W., E.O.P.-K., and I.A.R.; investigation, J.D.W. and G.F.S.W.; resources, J.D.W., E.O.P.-K., G.F.S.W., and I.A.R.; writing – original draft, J.D.W.; writing – reviewing & editing, J.D.W., E.O.P.-K., G.F.S.W., and I.A.R.; visualization, J.D.W.; supervision, I.A.R.; funding acquisition, G.F.S.W. and I.A.R.

DECLARATION OF INTERESTS

E.O.P.-K. is a cofounder of Xyme and holds a visiting professorship at the University of Liverpool.

SUPPLEMENTAL INFORMATION

Supplemental information can be found online at https://doi.org/10.1016/j.xcrp.2025.102404.

Received: October 21, 2024
Revised: December 5, 2024
Accepted: January 6, 2025
Published: January 28, 2025

REFERENCES

1. Almazrouei, B., Islayem, D., Alskafi, F., Catacutan, M.K., Amna, R., Nasrat, S., Sizirici, B., and Yildiz, I. (2023). Steroid hormones in wastewater: Sources, treatments, environmental risks, and regulations. Emerging Contam. *9*, 100210. https://doi.org/10.1016/j.emcon.2023.100210.
2. Wojnarowski, K., Podobiński, P., Cholewińska, P., Smoliński, J., and Dorobisz, K. (2021). Impact of Estrogens Present in Environment on Health and Welfare of Animals. Animals *11*, 2152. https://doi.org/10.3390/ani11072152.
3. Li, W., Wang, S., Li, J., Wang, X., Fan, B., Gao, X., and Liu, Z. (2020). Development of aquatic life criteria for tonalide (AHTN) and the ecological risk assessment. Ecotoxicol. Environ. Saf. *189*, 109960. https://doi.org/10.1016/j.ecoenv.2019.109960.
4. Ojoghoro, J.O., Scrimshaw, M.D., and Sumpter, J.P. (2021). Steroid hormones in the aquatic environment. Sci. Total Environ. *792*, 148306. https://doi.org/10.1016/j.scitotenv.2021.148306.
5. Silva, S.S., Abranches, D.O., Pinto, A.S., Soares, B.P., Passos, H., Ferreira, A.M., and Coutinho, J.A.P. (2023). Solubility Enhancement of Hydrophobic Compounds in Aqueous Solutions Using Biobased Solvents as Hydrotropes. Ind. Eng. Chem. Res. *62*, 12021–12028. https://doi.org/10.1021/acs.iecr.3c01469.
6. Zhang, B., and Isaacs, L. (2014). Acyclic Cucurbit[n]uril-type Molecular Containers: Influence of Aromatic Walls on their Function as Solubilizing Excipients for Insoluble Drugs. J. Med. Chem. *57*, 9554–9563. https://doi.org/10.1021/jm501276u.
7. Lazar, A.I., Biedermann, F., Mustafina, K.R., Assaf, K.I., Hennig, A., and Nau, W.M. (2016). Nanomolar Binding of Steroids to Cucurbit[n]urils: Selectivity and Applications. J. Am. Chem. Soc. *138*, 13022–13029. https://doi.org/10.1021/jacs.6b07655.
8. Hanikel, N., and Yaghi, O.M. (2023). Extracting pharmaceuticals from water using metal–organic frameworks. Nat. Water *1*, 418–419. https://doi.org/10.1038/s44221-023-00084-7.
9. Cullen, W., Takezawa, H., and Fujita, M. (2019). Demethylenation of Cyclopropanes via Photoinduced Guest-to-Host Electron Transfer in an M_6L_4 Cage. Angew. Chem. Int. Ed. *58*, 9171–9173. https://doi.org/10.1002/anie.201904752.
10. Percástegui, E.G. (2022). Metal–organic cages against toxic chemicals and pollutants. Chem. Commun. *58*, 5055–5071. https://doi.org/10.1039/D2CC00604A.
11. Mal, P., Breiner, B., Rissanen, K., and Nitschke, J.R. (2009). White phosphorus is air-stable within a self-assembled tetrahedral capsule. Science *324*, 1697–1699. https://doi.org/10.1126/science.1175313.
12. Yamashina, M., Tsutsui, T., Sei, Y., Akita, M., and Yoshizawa, M. (2019). A polyaromatic receptor with high androgen affinity. Sci. Adv. *5*, eaav3179. https://doi.org/10.1126/sciadv.aav3179.
13. Riddell, I.A., Smulders, M.M.J., Clegg, J.K., and Nitschke, J.R. (2011). Encapsulation, storage and controlled release of sulfur hexafluoride from a metal–organic capsule. Chem. Commun. *47*, 457–459. https://doi.org/10.1039/C0CC02573A.
14. Zhang, D., Ronson, T.K., Zou, Y.Q., and Nitschke, J.R. (2021). Metal-organic cages for molecular separations. Nat. Rev. Chem *5*, 168–182. https://doi.org/10.1038/s41570-020-00246-1.
15. Sun, Y., Chen, C., and Stang, P.J. (2019). Soft Materials with Diverse Suprastructures via the Self-Assembly of Metal–Organic Complexes. Acc. Chem. Res. *52*, 802–817. https://doi.org/10.1021/acs.accounts.8b00663.
16. Tranchemontagne, D.J., Ni, Z., O'Keeffe, M., and Yaghi, O.M. (2008). Reticular chemistry of metal-organic polyhedra. Angew. Chem. Int. Ed. *47*, 5136–5147. https://doi.org/10.1002/anie.200705008.
17. Martín Díaz, A.E., and Lewis, J.E.M. (2021). Structural Flexibility in Metal-Organic Cages. Front. Chem. *9*, 706462. https://doi.org/10.3389/fchem.2021.706462.
18. Riddell, I.A., Ronson, T.K., Clegg, J.K., Wood, C.S., Bilbeisi, R.A., and Nitschke, J.R. (2014). Cation- and anion-exchanges induce multiple distinct rearrangements within metallosupramolecular architectures. J. Am. Chem. Soc. *136*, 9491–9498. https://doi.org/10.1021/ja504748g.
19. Piskorz, T.K., Martí-Centelles, V., Spicer, R.L., Duarte, F., and Lusby, P.J. (2023). Picking the lock of coordination cage catalysis. Chem. Sci. *14*, 11300–11331. https://doi.org/10.1039/D3SC02586A.
20. Nakamura, T., Kaneko, Y., Nishibori, E., and Nabeshima, T. (2017). Molecular recognition by multiple metal coordination inside wavy-stacked macrocycles. Nat. Commun. *8*, 129. https://doi.org/10.1038/s41467-017-00076-8.
21. An, D., Shi, L., Li, T., Zhang, H.-Y., Chen, Y., Hao, X.-Q., and Song, M.-P. (2023). Tailored Supramolecular Cage for Efficient Bio-Labeling. Int. J. Mol. Sci. *24*, 2147. https://doi.org/10.3390/ijms24032147.

Please cite this article in press as: Wright et al., Encapsulation of hydrophobic pollutants within a large water-soluble $[Fe_4L_6]^{4-}$ cage, Cell Reports Physical Science (2025), https://doi.org/10.1016/j.xcrp.2025.102404

22. Sun, Q. (2022). The Hydrophobic Effects: Our Current Understanding. Molecules *27*, 7009. https://doi.org/10.3390/molecules27207009.

23. Jiang, Z., Wang, T., Yuan, S., Wang, M., Qi, W., Su, R., and He, Z. (2020). A tumor-sensitive biological metal–organic complex for drug delivery and cancer therapy. J. Mater. Chem. B *8*, 7189–7196. https://doi.org/10.1039/D0TB00599A.

24. Chen, J., Zhang, Y., Meng, Z., Guo, L., Yuan, X., Zhang, Y., Chai, Y., Sessler, J.L., Meng, Q., and Li, C. (2020). Supramolecular combination chemotherapy: a pH-responsive co-encapsulation drug delivery system. Chem. Sci. *11*, 6275–6282. https://doi.org/10.1039/D0SC01756F.

25. Geng, W.C., Ye, Z., Zheng, Z., Gao, J., Li, J.J., Shah, M.R., Xiao, L., and Guo, D.S. (2021). Supramolecular Bioimaging through Signal Amplification by Combining Indicator Displacement Assay with Förster Resonance Energy Transfer. Angew. Chem. Int. Ed. *60*, 19614–19619. https://doi.org/10.1002/anie.202104358.

26. Fujita, M., Yazaki, J., and Ogura, K. (1990). Preparation of a macrocyclic polynuclear complex, $[(en)Pd(4,4'\text{-}bpy)]_4(NO_3)_8$ (en = ethylenediamine, bpy = bipyridine), which recognizes an organic molecule in aqueous media. J. Am. Chem. Soc. *112*, 5645–5647. https://doi.org/10.1021/ja00170a042.

27. Stang, P.J., and Olenyuk, B. (1997). Self-Assembly, Symmetry, and Molecular Architecture: Coordination as the Motif in the Rational Design of Supramolecular Metallacyclic Polygons and Polyhedra. Acc. Chem. Res. *30*, 502–518. https://doi.org/10.1021/ar9602011.

28. Percástegui, E.G., Mosquera, J., Ronson, T.K., Plajer, A.J., Kieffer, M., and Nitschke, J.R. (2019). Waterproof architectures through subcomponent self-assembly. Chem. Sci. *10*, 2006–2018. https://doi.org/10.1039/C8SC05085F.

29. Taylor, L.L.K., Riddell, I.A., and Smulders, M.M.J. (2019). Self-Assembly of Functional Discrete Three-Dimensional Architectures in Water. Angew. Chem. Int. Ed. *58*, 1280–1307. https://doi.org/10.1002/anie.201806297.

30. Mecozzi, S., and Rebek Jr, J. (1998). The 55 % Solution: A Formula for Molecular Recognition in the Liquid State. Chem. Eur J. *4*, 1016–1022. https://doi.org/10.1002/(SICI)1521-3765(19980615)4:6<1016::AID-CHEM1016>3.0.CO;2-B.

31. Percástegui, E.G., Ronson, T.K., and Nitschke, J.R. (2020). Design and Applications of Water-Soluble Coordination Cages. Chem. Rev. *120*, 13480–13544. https://doi.org/10.1021/acs.chemrev.0c00672.

32. Mal, P., Schultz, D., Beyeh, K., Rissanen, K., and Nitschke, J.R. (2008). An unlockable-relockable iron cage by subcomponent self-assembly. Angew. Chem. Int. Ed. *47*, 8297–8301. https://doi.org/10.1002/anie.200803066.

33. Ma, D., Hettiarachchi, G., Nguyen, D., Zhang, B., Wittenberg, J.B., Zavalij, P.Y., Briken, V., and Isaacs, L. (2012). Acyclic cucurbit[n]uril molecular containers enhance the solubility and bioactivity of poorly soluble pharmaceuticals. Nat. Chem. *4*, 503–510. https://doi.org/10.1038/nchem.1326.

34. Ronson, T.K., Meng, W., and Nitschke, J.R. (2017). Design Principles for the Optimization of Guest Binding in Aromatic-Paneled $Fe^{II}{}_4L_6$ Cages. J. Am. Chem. Soc. *139*, 9698–9707. https://doi.org/10.1021/jacs.7b05202.

35. Carr, P.W., Stoll, D.R., and Wang, X. (2011). Perspectives on Recent Advances in the Speed of High Performance Liquid Chromatography. Anal. Chem. *83*, 1890–1900. https://doi.org/10.1021/ac102570t.

36. Caulder, D.L., Powers, R.E., Parac, T.N., and Raymond, K.N. (1998). The Self-Assembly of a Predesigned Tetrahedral M_4L_6 Supramolecular Cluster. Angew. Chem. Int. Ed. *37*, 1840–1843. https://doi.org/10.1002/(SICI)1521-3773(19980803)37:13/14<1840::AID-ANIE1840>3.0.CO;2-D.

37. Meng, W., Clegg, J.K., Thoburn, J.D., and Nitschke, J.R. (2011). Controlling the Transmission of Stereochemical Information through Space in Terphenyl-Edged Fe_4L_6 Cages. J. Am. Chem. Soc. *133*, 13652–13660. https://doi.org/10.1021/ja2055254s.

38. Clegg, J.K., Cremers, J., Hogben, A.J., Breiner, B., Smulders, M.M.J., Thoburn, J.D., and Nitschke, J.R. (2013). A stimuli responsive system of self-assembled anion-binding $Fe_4L_6{}^{8+}$ cages. Chem. Sci. *4*, 68–76. https://doi.org/10.1039/C2SC21486E.

39. Rigaku Oxford Diffraction (2024). CrysAlisPro Software System (Rigaku Corporation) version 1.171.43.116a.

40. Kleywegt, G.J., and Jones, T.A. (1994). Detection, delineation, measurement and display of cavities in macromolecular structures. Acta Crystallogr. *50*, 178–185. https://doi.org/10.1107/S0907444993011333.

41. Bhandari, R.K., Deem, S.L., Holliday, D.K., Jandegian, C.M., Kassotis, C.D., Nagel, S.C., Tillitt, D.E., Vom Saal, F.S., and Rosenfeld, C.S. (2015). Effects of the environmental estrogenic contaminants bisphenol A and 17alpha-ethinyl estradiol on sexual development and adult behaviors in aquatic wildlife species. Gen. Comp. Endocrinol. *214*, 195–219. https://doi.org/10.1016/j.ygcen.2014.09.014.

42. Ghosh, A., Pruchyathamkorn, J., Espinosa, C.F., and Nitschke, J.R. (2024). Light-Driven Purification of Progesterone from Steroid Mixtures Using a Photoresponsive Metal–Organic Capsule. J. Am. Chem. Soc. *146*, 2568–2574. https://doi.org/10.1021/jacs.3c11005.

43. Aris, P., Wei, Y., Mohamadzadeh, M., and Xia, X. (2022). Griseofulvin: An Updated Overview of Old and Current Knowledge. Molecules *27*, 7034. https://doi.org/10.3390/molecules27207034.

44. Johnson, M. (1995). The anti-inflammatory profile of fluticasone propionate. Allergy *50*, 11–14. https://doi.org/10.1111/j.1398-9995.1995.tb02735.x.

45. Metherell, A.J., Cullen, W., Williams, N.H., and Ward, M.D. (2018). Binding of Hydrophobic Guests in a Coordination Cage Cavity is Driven by Liberation of "High-Energy" Water. Chem. Eur J. *24*, 1554–1560. https://doi.org/10.1002/chem.201704163.

46. Biedermann, F., Uzunova, V.D., Scherman, O.A., Nau, W.M., and De Simone, A. (2012). Release of High-Energy Water as an Essential Driving Force for the High-Affinity Binding of Cucurbit[n]urils. J. Am. Chem. Soc. *134*, 15318–15323. https://doi.org/10.1021/ja30330.